論文 96-1-1-14

Performance Analysis of Maximum-Likelihood Code Acquisition Technique for Preamble Search in CDMA Reverse Link

Hyung-Rae Park*, Bub-Joo Kang* Regular Members

CDMA 역방향 링크에서의 프리앰블 탐색을 위한 최대우도 동기획득 방식의 성능 분석

正會員 朴 亨 來*, 康 法 周*

ABSTRACT

Addressed in this paper is a performance analysis of the maximum-likelihood code acquisition technique for slotted-mode preamble search in the CDMA reverse link.

The probabilities of detection, miss, and false alarm are derived analytically for a multiple H_1 cell case in a frequency-selective Rayleigh fading channel, based on the statistics of the CDMA noncoherent demodulator output. The probability density function of the decision variable consisting of successive demodulator outputs is also derived by considering the fading characteristics of the received signal for both single and dual antenna cases.

The performance of the code acquisition technique is evaluated numerically with an emphasis on investigating the effects of post-detection integration, fading rate, and antenna diversity on the detection performance.

要 約

CDMA 역방향 링크에서 슬롯 모드로 전송되는 프리앰블을 탐색하기 위한 최대우도 동기획득 방식의 성능을 분석한다.

CDMA 복조기 출력의 통계적 특성에 기초하여 신호검출 성능을 주파수 선택성 레일라이 페이딩 채널에서 다중 H_1 셀의 경우에 대해 이론적으로 분석한다. 복조기 출력으로 구성되는 판정 변수의 확률밀도 함수를 수신신호의 페이딩 특성을 고려하여 단일 및 이중 안테나 시스템의 경우에 대해 유도하고 후치 적분의 수, 페이딩 율 및, 안테나 다이버시티에 따른 효과를 고려하여 성능을 분석한다.

* 한국전자통신연구소 이동통신연구단 신호처리연구실
論文番號 : 95193-0529
接受日字 : 1995年 5月 29日

Ⅰ. Introduction

Recently, direct-sequence spread spectrum (DS-SS) technique has attracted much attention for mobile communication applications, so called the code division multiple access (CDMA) system, which has been shown to have significant advantages over conventional analog FM or time division multiple access (TDMA) system [1]-[3]. However, like other spread spectrum applications, the advantages of the CDMA system can be exploited only in case where the pseudo-noise (PN) sequences of the local generator and the received signal are synchronized within a small fraction of one PN chip. In general, the code synchronization process in spread spectrum systems consists of two steps, code acquisition (coarse alignment) and code tracking (fine alignment), of which the former is dealt with in this paper.

The performance of the maximum-likelihood (ML) code acquisition technique [4], [5] is analyzed for slotted-mode preamble search in the CDMA reverse link (mobile-to-base station) in a frequency-selective Rayleigh fading channel. Although the acquisition process in the reverse link can be divided into the initial code acquisition for locating the H_1 region or one of the H_1 cells and the multipath search for finding stronger paths over the H_1 region, our analysis is focused on the former case. For code acquisition in the reverse link, the mobile, in general, transmits a preamble (unmodulated PN sequence) preceding the access slot message, which has been aligned with the pilot signal through the code acquisition in the forward link (base station-to-mobile). At the base station, the code phase of the signal transmitted by the mobile is retarded by round-trip-delay compared with that of the pilot signal. Therefore, the uncertainty region where the code phase of the received signal may be located is quite small in the reverse link, depending on the maximum distance between the base station and the mobile. In the forward link, the uncertainty region is a full period of PN sequence. Since the probability of detection (or acquisition) for a certain access slot transmitted by the mobile is more desirable than the mean acquisition time as a performance measure, the ML technique which is the optimum at the viewpoint of the detection probability may be better than the serial or sequential techniques [6]-[8] for slotted-mode preamble search. It is, however, well known that the serial or sequential techniques provide the better performance than the ML technique in case of pilot acquisition in the CDMA forward link where the mean acquisition time is more important performance measure [9].

So far, the performance of the code acquisition techniques has been discussed mostly with the assumptions that there is a single H_1 cell [4]-[8] over the uncertainty region and that there is no correlation between successive demodulator outputs forming the decision variable over the period of post-detection integration. However, since there exist multiple H_1 cells in real mobile communication environments, due to the search step size smaller than one PN chip (typically 1/2 PN chips) and the delay spread of the received signal, the single H_1 cell approaches show the code acquisition performance significantly poorer than as it would be. In addition, the successive demodulator outputs at the H_1 cells are highly correlated over the period of post-detection integration, in which the degree of correlation depends on the fading rate of the signal. Obviously, the correlation between

successive demodulator outputs provides a detection performance significantly worse than the case without correlation.

In this paper, the probabilities of detection, miss, and false alarm are derived analytically for a multiple H_1 cell case in a frequency-selective Rayleigh fading channel, based on the statistics of the CDMA noncoherent demodulator output. The probability density function (pdf) of the decision variable is also derived by considering the fading characteristics of the signal to address the effect of fading rate. Since the antenna diversity is employed generally in the base station to increase the channel capacity in the reverse link, it may be interesting to examine its potential to improve the code acquisition performance. The performance of the ML technique is evaluated numerically for slotted-mode preamble search in the CDMA reverse link, with an emphasis on investigating the effects of post-detection integration, fading rate, and antenna diversity on the code acquisition performance.

This paper is organized as follows. In section Ⅱ, a serial-parallel implementation of the ML technique is described together with an analytical derivation of the mean acquisition time. The detection, miss, and false alarm probabilities are derived in a frequency-selective Rayleigh fading channel in section Ⅲ, by taking into account the correlation between successive demodulator outputs for both single and dual antenna cases. In section Ⅳ, the performance of the ML technique is evaluated numerically, followed by conclusion in section Ⅴ.

Ⅱ. System Description

A serial-parallel implementation of the ML code acquisition system is described in Figure 1, which consists of N_p parallel I/Q correlators. The search window size in the reverse link, defined as the uncertainty region, is determined by the maximum distance between the base station and the mobile. That is, the search window size, N_w, is given by

$$N_w = \frac{2\ell_m}{cT_c}, \tag{1}$$

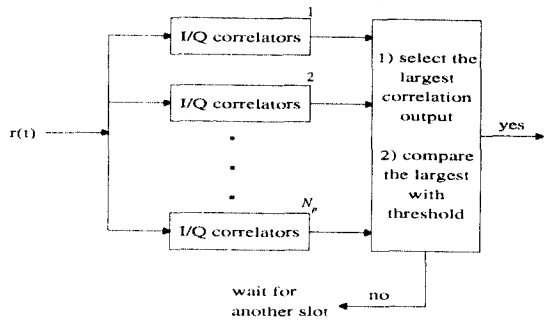

Fig. 1. A serial-parallel implementation of the ML code acquisition system.

where ℓ_m and c are the maximum distance and the speed of light, respectively, and T_c denotes the PN chip duration. Since the search step size, Δ, is generally less than one PN chip, the number of total test cells over the whole uncertainty region is given by N_w/Δ, where Δ is defined with the PN chip unit. In order to reduce the total processing time for obtaining the correlator outputs at all test cells, the search window is divided into N_p sub-windows, of which each sub-window is covered by the corresponding I/Q correlator. In this case, the total processing time is given by

$$T = N_w\tau_D/(\Delta N_p), \tag{2}$$

where τ_D is the processing time required for

obtaining a correlator output at each test cell. The number of I/Q correlators should be selected by considering the system complexity and the total processing time. In case where dual antennas are employed, half of the I/Q correlators is assigned to antenna 'A' and the other half to antenna 'B', so that the search window is divided into $N_p/2$ sub-windows.

If the largest among all correlator outputs is greater than the decision threshold, the correponding code phase is accepted tentatively as the true one of the received signal. Otherwise, the system waits for the next slot. In case where the correlator output at one of the H_1 cells is the largest and greater than the decision threshold, the system is said to have acquired the code phase of the signal. On the contrary, if the largest greater than the threshold corresponds to one of the H_0 cells, it is said that false alarm has occurred. Most code acquisition systems employ the verification mode to confirm whether the tentative H_1 decision is true or not [4]-[7]. However, we herein consider the single-dwell system without verification mode since an equivalent verification may be obtained by error handling technique (for example, cyclic redundancy check) for slotted-mode preamble search [10]. The single-dwell ML code acquisition technique can be described by the state diagram as shown in Figure 2. In the figure, P_D, P_M, and P_F denote the probabilities of detection, miss, and false alarm, which are defined as

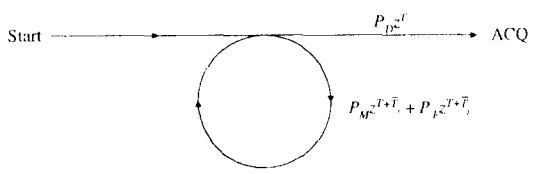

Fig. 2. State diagram.

P_D = Pr{one of the correlator outputs at the H_1 cells is the largest and greater than threshold},

P_M = Pr{none of the correlator outputs is greater than threshold},

P_F = Pr{one of the correlator outputs at the H_0 cells is the largest and greater than threshold}. (3)

$\bar{T}_p$ and $\bar{T}_r$ represent the average penalty time for 'returning' false alarm [6] and the average reset time for miss, respectively, which are generally equivalent in the reverse link. A typical example of the access slot structure transmitted by the mobile is shown in Figure 3, which illustrates the relationships among the processing time, reset time, preamble size, message size, and so on [10]. Since the access slots are transmitted at random time intervals (that is, $T_{w,i}$ is random), the reset and penalty times are random variables. Of course, the processing time, T, should be selected smaller than the preamble size, T_{pre}. The transfer function of the state diagram is simply obtained as

$$U(z) = \frac{P_D z^T}{1 - \left(P_M z^{T+\bar{T}_r} + P_F z^{T+\bar{T}_p}\right)}. \quad (4)$$

The mean acquisition time is therefore given by

$$E[T_{acq}] = \left.\frac{dU(z)}{dz}\right|_{z=1} = \frac{T + \bar{T}_r(1-P_D)}{P_D}. \quad (5)$$

where $\bar{T}_p = \bar{T}_r$ and $P_D + P_M + P_F = 1$ have been used.

Ⅲ. Detection Performance of ML Code Acquisition Technique

A. Statistics of Noncoherent Demodulator

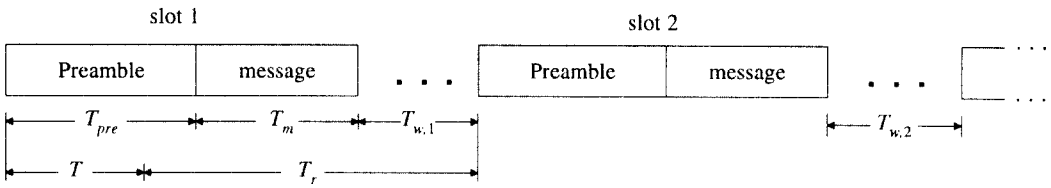

Fig. 3. A typical example of access slot structure.

Output in Frequency-Selective Rayleigh Fading Channel

The statistics of the noncoherent demodulator output in asynchronous CDMA system is discussed in the Appendix for a deterministic signal case. We now consider the more general case where q signals arrive at the receiver with different time delays over frequency-selective Rayleigh fading channel. The tapped-delay line model shall be used for characterizing the wideband fading channel such that the delay profile of the received signal be described by Dirac delta functions, defined with a relative time delay, τ_k, and weight of α_k^2, for $k = 1, 2, \ldots, q$ [11],[12]. The fading channel is assumed to be wide-sense stationary and uncorrelated for different time delays [13]. Based on the discussions in the Appendix, the I/Q correlator outputs at a H_1 cell can be written as

$$Y_I = N\sqrt{E_c}\sum_{k=1}^{q}\alpha_k R(\tau_{e,k})\cos\varphi_k + n_{I,N},$$
$$Y_Q = N\sqrt{E_c}\sum_{k=1}^{q}\alpha_k R(\tau_{e,k})\sin\varphi_k + n_{Q,N}, \quad (6)$$

with

$$R(\tau_{e,k}) \approx 0, \quad \text{for } |\tau_{e,k}| > T_c. \quad (7)$$

In the above equations, α_k and φ_k represent the envelope and phase of the signal in the k-th path, respectively, and $\tau_{e,k}$ denotes the timing error for the k-th signal at a H_1 cell under test. E_c and N are the signal energy per PN chip and the number of accumulated PN chips. The superscript 'i' used for denoting the *i-th* user in the Appendix has been omitted for convenience in notation. It should be noted that unlike the case in the Appendix, the subscript 'k' has been used to denote the signals in different paths all coming from the same user. $R(\cdot)$ is the convolution of the impulse responses of the pulse shaping filter and the matched filter which are assumed to be identical. Eq. (6) shows that the signal component at a certain H_1 cell is given by the superposition of the signals in different paths with a weight $R(\tau_{e,k})$. The envelopes of the signals are assumed to be independent of each other and to have the same fading characteristics. The I/Q noise components, $n_{I,N}$ and $n_{Q,N}$, represent the Gaussian noise processes with the variance of $NI_o/2$, where I_o is the power spectral density due to the inter-chip interference, other-user interference, and background noise. Based on the above discussions, the mean of Z, the squared sum of I/Q correlator outputs, is obtained as

$$E[Z] = E\left[Y_I^2 + Y_Q^2\right]$$
$$= N^2 E_c \sum_{k=1}^{q} E[\alpha_k^2] R^2(\tau_{e,k}) + NI_o$$
$$\equiv V_s + V_N, \quad (8)$$

with

$$V_s = N^2 E_c \sum_{k=1}^{q} E[\alpha_k^2] R^2(\tau_{e,k}) \tag{9}$$

and

$$V_N = NI_0. \tag{10}$$

Eq. (8) has been derived under the assumption that the envelopes and phases of the received signal are relatively constant over the coherent accumulation period of NT_c.

In order to improve the detection performance, it is, however, necessary to increase the observation period beyond the coherent accumulation period by taking the sum of successive demodulator outputs as the decision variable. In this case, the pdf of the decision variable becomes a function of the fading rate or equivalently autocorrelation function of the signal, which represents the short-term fading characteristics. The autocorrelation function in a Rayleigh fading channel has been discussed by several authors based on the scattering model [13]. The Clarke's two dimensional model which has been derived under the assumption that all scattered waves are confined to the horizontal plane shall be used in this paper to investigate the effect of fading rate. In [13], the normalized autocorrelation function of the signal is given by

$$r_s(\tau) = J_0(2\pi f_m \tau), \tag{11}$$

where $J_0(\cdot)$ is the zero-order Bessel function of the first kind and $f_m = v/\lambda$ is the maximum Doppler spread with v and λ denoting the speed of the mobile and wavelength, respectively.

B. Detection, Miss, and False Alarm Probabilities

We herein derive the detection, miss, and false alarm probabilities of the ML code acquisition technique described in section Ⅱ. Assume that there are p H_1 cells. Then, the number of H_0 cells is $N_v - p$, where N_v is the number of total test cells. Under the assumption that the decision variable at each test cell is independent, the probability that the correlator output at the j-th H_1 cell is the largest and greater than the decision threshold, η_0, is given by

$$P_{D,j} = \int_{\eta_0}^{\infty} \left\{ \left[\int_0^{\eta_j} f_\eta(\eta|H_0) d\eta \right]^{N_v - p} \prod_{\substack{i=1 \\ i \neq j}}^{p} \left[\int_0^{\eta_j} f_{\eta_i}(\eta_i|H_1) d\eta_i \right] \right\} f_{\eta_j}(\eta_j|H_1) d\eta_j, \tag{12}$$

where $f_\eta(\eta \mid H_0)$ and $f_{\eta_j}(\eta_j \mid H_1)$ denote the pdfs of the decision variables under hypotheses H_0 and H_1, respectively. The subscript 'j' has been used to denote the decision variable at the j-th H_1 cell. For a general case of multiple H_1 cells, each H_1 cell contributes to the detection probability. Therefore, the detection probability considering all the H_1 cells is given by

$$\begin{aligned} P_D &= \sum_{j=1}^{p} P_{D,j} \\ &= \sum_{j=1}^{p} \int_{\eta_0}^{\infty} \left\{ \left[\int_0^{\eta_j} f_\eta(\eta|H_0) d\eta \right]^{N_v - p} \prod_{\substack{i=1 \\ i \neq j}}^{p} \left[\int_0^{\eta_j} f_{\eta_i}(\eta_i|H_1) d\eta_i \right] \right\} f_{\eta_j}(\eta_j|H_1) d\eta_j. \end{aligned} \tag{13}$$

The miss and false alarm probabilities are also easily obtained as

$$\begin{aligned} P_M &= \left[\int_0^{\eta_0} f_\eta(\eta|H_0) d\eta \right]^{N_v - p} \prod_{i=1}^{p} \left[\int_0^{\eta_0} f_{\eta_i}(\eta_i|H_1) d\eta_i \right], \\ P_F &= 1 - P_D - P_M. \end{aligned} \tag{14}$$

Using Eqs. (13) and (14), we may analyze the detection performance of the ML code acquisition technique by inserting the pdfs of the decision variables into them.

C. Derivation of Probability Density Function

The pdf of the decision variable is derived analytically by considering the fading characteristics of the signal. Two cases are considered, one for single antenna case and the other for dual antenna case.

1) Case 1 (single antenna case) : The decision variable for single antenna case is given by

$$\eta = \sum_{\ell=1}^{L} Z_\ell. \tag{15}$$

Under hypothesis H_0, since the random variable, $2\eta/V_N$, has a central χ^2 distribution with $2L$ degrees of freedom, the pdf of η is given by

$$f_\eta(\eta|H_0) = \frac{1}{(L-1)!V_N^L}\eta^{L-1}\exp(-\eta/V_N). \tag{16}$$

In order to derive the pdf of η under hypothesis H_1, define a complex Gaussian random vector, $\mathbf{x}$, whose elements consist of I/Q correlator outputs, each corresponding to the real and imaginary parts of the complex random variable, x_ℓ, $\ell = 1, 2, \ldots, L$, respectively. That is,

$$\mathbf{x} = (x_1, x_2, \ldots, x_L)^T, \tag{17}$$

where the superscript 'T' denotes the transpose operator. Then, the decision variable can be represented as a quadratic form of $\mathbf{x}$ as follow,

$$\eta = \mathbf{x}^H\mathbf{x}, \tag{18}$$

with the superscript 'H' representing the Hermitian transpose. The covariance matrix of $\mathbf{x}$ can be represented as

$$\begin{aligned}\mathbf{R}_x &= E[\mathbf{x}\mathbf{x}^H] \\ &= \mathbf{R}_s + V_N\mathbf{I}_L,\end{aligned} \tag{19}$$

where $\mathbf{R}_s$ and $\mathbf{I}_L$ are the signal covariance matrix and $L\times L$ identity matrix for noise components, respectively. The signal covariance matrix represents the fading characteristics of the signal and can be expressed as

$$\mathbf{R}_s = V_s\begin{bmatrix} r_s(0) & r_s(NT_c) & \cdots & r_s((L-1)NT_c) \\ r_s(NT_c) & r_s(0) & \cdots & r_s((L-2)NT_c) \\ \vdots & \vdots & \ddots & \vdots \\ r_s((L-1)NT_c) & r_s((L-2)NT_c) & \cdots & r_s(0) \end{bmatrix} \tag{20}$$

where V_s and $r_s(\cdot)$ are defined by Eqs. (9) and (11). It has been assumed that the signal component is perfectly correlated over the coherent accumulation period of NT_c. Define a random vector $\mathbf{y} = \mathbf{R}_x^{-1/2}\mathbf{x}$, then

$$\begin{aligned}E[\mathbf{y}\mathbf{y}^H] &= \mathbf{R}_x^{-1/2}E[\mathbf{x}\mathbf{x}^H]\mathbf{R}_x^{-1/2} \\ &= \mathbf{I}_L,\end{aligned} \tag{21}$$

which shows that $\mathbf{y}$ is a complex Gaussian random vector with zero mean. Thus, the decision variable can be equivalently expressed as,

$$\begin{aligned}\eta &= \mathbf{y}^H\mathbf{R}_x\mathbf{y} \\ &= \sum_{\ell=1}^{L}\lambda_\ell|\omega_\ell|^2,\end{aligned} \tag{22}$$

where $\omega_\ell = \mathbf{u}_\ell^H\mathbf{y}$, $\ell = 1, 2, \ldots, L$, are complex Gaussian random variables each having the same unit variance and independent of each other. λ_ℓ and $\mathbf{u}_\ell$ are the ℓ-th eigenvalue and eigenvector of $\mathbf{R}_x$, respectively. Since $\mathbf{R}_x$ is positive definite, its eigenvalues are always positive. It should be noted that the decision variable, η, is a linear combination of the χ^2 random variables with 2 degrees of freedom. The pdf of η is therefore easily derived from the characteristic function of η, which is given by [14]

$$\begin{aligned}\Phi(t) &= E[\exp(j\eta t)] \\ &= \sum_{\ell=1}^{L}\frac{b_\ell}{(1-jt\lambda_\ell)},\end{aligned} \tag{23}$$

with

$$b_\ell = \lambda_\ell^{L-1}\prod_{\substack{i=1\\ i\neq\ell}}^{L}(\lambda_\ell-\lambda_i)^{-1}, \quad \ell = 1, 2, \ldots, L. \tag{24}$$

Eq. (23) has been obtained under the assumption that the eigenvalues are distinct of each other, which is generally true for a reasonable size of post-detection integration. Finally, the pdf of η under hypothesis H_1 is obtained by taking the inverse Fourier transform on Eq. (23), which is given by

$$f_\eta(\eta|H_1) = \sum_{\ell=1}^{L}\frac{b_\ell}{\lambda_\ell}\exp(-\eta/\lambda_\ell). \tag{25}$$

2) Case 2 (dual antenna case)

In the CDMA system, the base station generally employs dual antennas to increase the channel capacity in the reverse link through antenna diversity. We now derive the pdf of the decision variable for dual antenna case to investigate the potential of the antenna diversity to improve the code acquisition performance. In order to utilize the dual antenna diversity, the correlator outputs from both antennas are summed to form the decision variable, which can be expressed as

$$\eta = \sum_{\ell=1}^{L}Z_{A,\ell} + \sum_{\ell=1}^{L}Z_{B,\ell}. \tag{26}$$

The subscripts 'A' and 'B' denote the correlator outputs from antenna 'A' and 'B', respectively. Under hypothesis H_0, the pdf of η is easily derived as

$$f_\eta(\eta|H_0) = \frac{1}{(2L-1)!V_N^{2L}}\eta^{2L-1}\exp(-\eta/V_N). \tag{27}$$

Under hypothesis H_1, following the same procedures as in Case 1, we can express the decision variable as

$$\eta = \sum_{\ell=1}^{L}\lambda_\ell|\omega_\ell|^2 + \sum_{\ell=1}^{L}\lambda_\ell|v_\ell|^2, \tag{28}$$

where ω_ℓ and v_ℓ are complex Gaussian random variables each having the same unit variance and independent of each other. Thus, the characteristic function of η is

$$\Phi(t) = E[\exp(jt\eta)] = \sum_{\ell=1}^{L}\frac{b_\ell}{(1-jt\lambda_\ell)} + \sum_{\ell=1}^{L}\frac{c_\ell}{(1-jt\lambda_\ell)^2}, \tag{29}$$

with

$$b_\ell = \sum_{\substack{k=1\\ k\neq\ell}}^{L}\frac{-2\lambda_k}{\lambda_\ell-\lambda_k}\prod_{\substack{j=1\\ j\neq\ell}}^{L}\left[\frac{\lambda_\ell^2}{(\lambda_\ell-\lambda_j)^2}\right]$$

$$c_\ell = \prod_{\substack{j=1\\ j\neq\ell}}^{L}\left[\frac{1}{(1-\lambda_j/\lambda_\ell)^2}\right], \quad \ell = 1, 2, \ldots, L. \tag{30}$$

It follows that $b_\ell = 0$ and $c_\ell = 1$ in the above equation for the case of L=1. The pdf of η under hypothesis H_1 is therefore given by

$$f_\eta(\eta|H_1) = \sum_{\ell=1}^{L}\frac{b_\ell}{\lambda_\ell}\exp(-\eta/\lambda_\ell) + \sum_{\ell=1}^{L}\frac{\eta c_\ell}{\lambda_\ell^2}\exp(-\eta/\lambda_\ell). \tag{31}$$

Ⅳ. Numerical Results and Discussions

In this section, the performance of the ML code acquisition technique described in section Ⅱ shall be evaluated numerically for slotted-mode preamble search in the CDMA reverse link. The period of I/Q PN sequences and the PN chip rate are assumed to be 2^{15} and 1.2288 MHz, respectively. The search window size is taken to be 164 PN chips throughout the evaluations with the assumption that the maximum distance between the base station and the mobile, ℓ_m, is 20 km. The search step size is set to 1/2. Three signals are assumed to arrive at intervals of 1 PN chip over frequency-selective Rayleigh fading channel. In this case, the numbers of H_1 and H_0 cells are 8 and 320, respectively. The energy of each

signal is taken to be 0.57, 0.29, and 0.14 times the total signal energy, respectively, which is a typical example of the fading channel in urban areas. The demodulator outputs $Z_{A,\ell}$ and $Z_{B,\ell}$ are obtained by accumulating the output samples over 256 PN chips (that is, N = 256), which is a reasonable selection in real mobile communication environments. Note that the signal energy at the demodulator output is proportional to $R^2(\tau_e)$ in Eq. (9), where τ_e is a timing error. With a pulse shaping filter for band-limiting the power spectral density of the signal, $R(\tau_e)$ may be approximated to the sinc function

$$R(\tau_e)=\frac{\sin(\pi\tau_e/T_c)}{\pi\tau_e/T_c}, \tag{32}$$

which shall be used for calculating the signal loss due to the timing error. Unless specified otherwise, all numerical examples are given for dual antenna case, and the signal-to-noise ratio per PN chip, SNR_c, and the maximum Doppler spread, f_m, are set to -16 dB and 50 Hz, respectively. The minimum timing error between the code phases of the signals and the test cell is assumed to be $\pm\triangle/2\ T_c$. After coherent accumulation over 256 PN chips, the total signal-to-noise ratio becomes 8.1 dB. Figure 4 shows the effect of post-detection integration on the probability of detection. As expected, the detection performance is improved significantly as the number of post-detection integration is increased. This is simply due to the fact that the degree of freedom of the decision variable becomes larger as the number of post-detection integration is increased. It is also seen that the probability of detection of the ML code acquisition technique is quite insensitive to the decision threshold unlike the serial or sequential techniques [6]~[8] whose decision is made on a cell-by-cell basis. In order to have the probability of detection greater than 0.95 for a given condition, it is necessary to select the number of post-detection integration larger than 2. Figure 5 illustrates the effect of post-detection integration in terms of the mean acquisition time. It is selected that N_p = 12, T_m = 60 milli-seconds (*ms*), $\overline{T}_w$ = 200 *ms*. The processing time, T_c in this example is

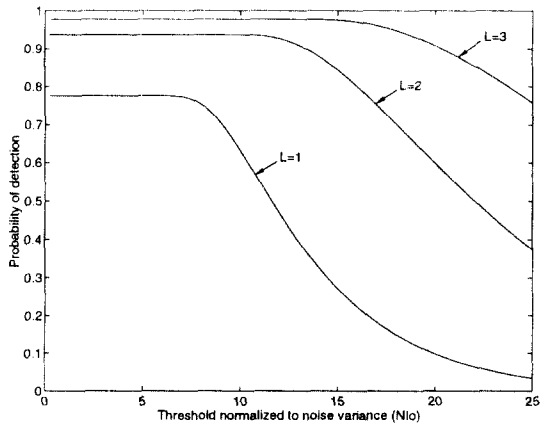

Fig. 4. Effect of post-detection integration on the probability of detection.

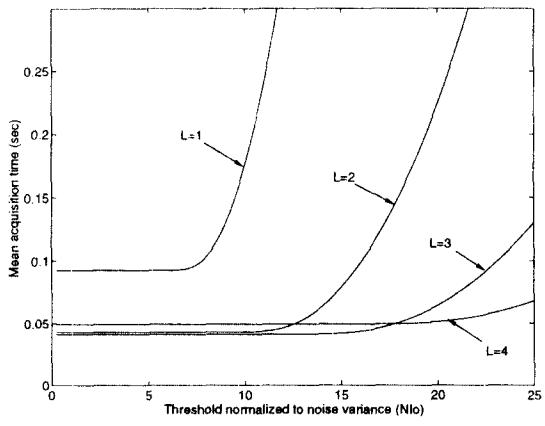

Fig. 5. Effect of post-detection integration on the mean acquisition time.

given by $11.4 \times L$ *ms*. The preamble size, T_{pre}, is set to the smallest integer multiple of 20 *ms*, and at least, greater than the processing time. Therefore, the preamble sizes are 20 *ms* for L=1, 40 *ms* for L=2 and 3, and 60 *ms* for L=4, respectively. The average reset or penalty times are 268.6, 277.2, 265.8, and 274.4 *ms* for L = 1~4, respectively. It is observed in the figure that L=3 is an optimal selection for a given condition at the viewpoint of the mean acquisition time. This observation may be explained as follow. Although the detection probability becomes high as the number of post-detection integration is increased, the increase in the processing time overwhelms the benefit in the detection probability for the case of L greater than 3. It is also seen that the mean acquisition time for L=4 is less than that for L=2 or 3 in case where the decision threshold is set too large such that the improvement of the detection performance is more significant than the increase in the processing time. Figure 6 shows the effect of Doppler spread or fading rate on the probability of detection for L=3. It is seen in the figure that the probability of detection is not affected significantly by Doppler spread of the signal, which means that Doppler spread due to the user's mobility does not provide the time diversity efficiently in real mobile communication environments. Figure 7 illustrates the effect of dual antenna diversity on the code acquisition performance. The dotted curves represent the probability of detection in case where a single antenna is used. In this case, the number of post-detection integration is doubled since all the I/Q correlators are assigned to antenna '*A*' or '*B*'. It is observed in the figure that the probability of detection in the dual antenna case is significantly higher than that in the single antenna case, which is due to the fact that utilizing dual antennas provides the diversity effect more efficiently than increasing the period of post-detection integration.

Ⅴ. Conclusion

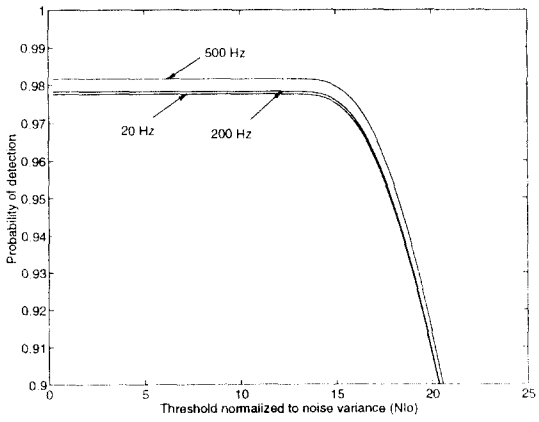

Fig. 6. Effect of Doppler spread on the probability of detection.

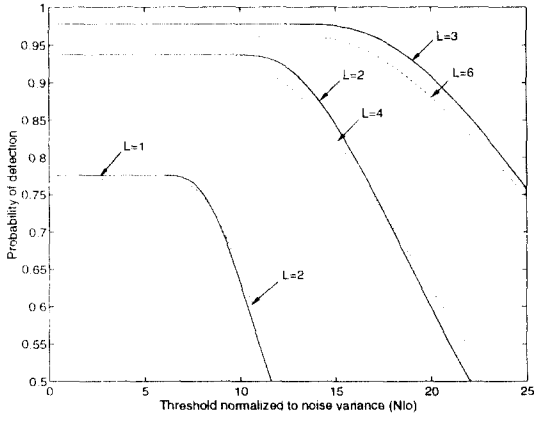

Fig. 7. Effect of antenna diversity on the probability of detection.

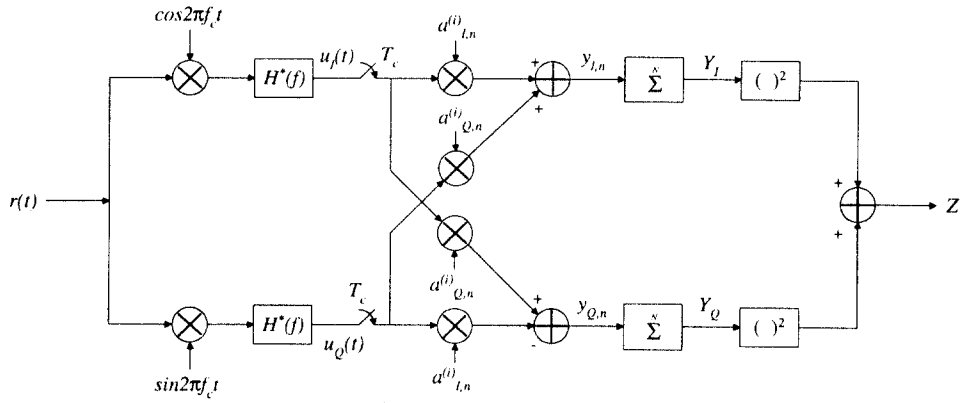

Fig. 8. Simplified noncoherent QPSK demodulator.

In this paper, the performance of the ML code acquisition technique has been analyzed for slotted-mode preamble search in the CDMA reverse link in a frequency-selective Rayleigh fading channel. The probabilities of detection, miss, and false alarm have been derived analytically for a multiple H_1 cell case, based on the statistics of the CDMA noncoherent demodulator output. The pdf of the decision variable has been also derived by considering the fading characteristics of the signal for both single and dual antenna cases. The performance of the ML technique has been evaluated numerically, with an emphasis on investigating the effects of post-detection integration, fading rate, and antenna diversity on the code acquisition performance.

It has been shown in the numerical examples that while increasing the number of post-detection integration improves the detection performance significantly, there is an optimum value for the size of post-detection integration in terms of the mean acquisition time, which is 3 for a given example. It has been also observed that the fading rate due to the user's mobility hardly affects the code acquisition performance since it does not provide the time diversity efficiently in mobile communication environments. The example for examining the effect of antenna diversity has shown that the probability of detection in the dual antenna case is significantly higher than that in the single antenna case. It is also interesting to note that the detection performance of the ML code acquisition technique is quite insensitive to threshold setting unlike the serial or sequential techniques unless the decision threshold is set to an extremely high value.

Appendix. Statistics of Noncoherent Demodulator Output in Asynchronous CDMA System

We herein discuss the statistics of the noncoherent demodulator output in asynchronous CDMA system for a deterministic signal case. A simplified noncoherent QPSK demodulator representing only the basic processes of signal

despreading and matched filtering is described in Figure 8. The signal is assumed to be modulated by balanced QPSK scheme [15]. The transmitted signal by the *i-th* user can be written as [15]

$$s^{(i)}(t)=\sqrt{E_c^{(i)}}\cos(2\pi f_c t)\sum_m x_m^{(i)}a_{I,m}^{(i)}h(t-mT_c)+\sqrt{E_c^{(i)}}\sin(2\pi f_c t)\sum_m x_m^{(i)}a_{Q,m}^{(i)}h(t-mT_c), \tag{33}$$

where $E_c^{(i)}$ and $h(t)$ represent the signal energy per PN chip and the impulse response of the pulse shaping filter. $x_m^{(i)}$ is the information sequence which is constant over an information bit duration, and $a^{(i)}_{I,m}$ and $a^{(i)}_{Q,m}$ represent I/Q PN sequences for spreading the signal. f_c is the carrier frequency. Ignoring the signal attenuation due to the propagation loss, the received signal at the base station from N_u users is given by

$$r(t)=\sum_{j=1}^{N_u}\sqrt{E_c^{(j)}}\cos(2\pi f_c t+\varphi_j)\sum_m x_m^{(j)}a_{I,m}^{(j)}h(t-mT_c-\tau_j)+\sum_{j=1}^{N_u}\sqrt{E_c^{(j)}}\sin(2\pi f_c t+\varphi_j)\sum_m x_m^{(j)}a_{Q,m}^{(j)}h(t-mT_c-\tau_j)+n_I(t)\cos(2\pi f_c t)-n_Q(t)\sin(2\pi f_c t), \tag{34}$$

where $n_I(t)$ and $n_Q(t)$ are narrowband Gaussian noise processes due to the background or thermal noise each having a double-sided spectral density of N_o. φ_j and τ_j represent the phase and relative time delay of the signal transmitted by the *j-th* user. The I/Q channel outputs of the matched filter for the *i-th* user are

$$u_I(t)=\frac{1}{2}\sum_{j=1}^{N_u}\sqrt{E_c^{(j)}}\sum_m x_m^{(j)}\left\{\cos\varphi_j a_{I,m}^{(j)}+\sin\varphi_j a_{Q,m}^{(j)}\right\}R(t-mT_c-\tau_j)+\frac{1}{2}n_I'(t) \tag{35}$$

and

$$u_Q(t)=\frac{1}{2}\sum_{j=1}^{N_u}\sqrt{E_c^{(j)}}\sum_m x_m^{(j)}\left\{\cos\varphi_j a_{Q,m}^{(j)}-\sin\varphi_j a_{I,m}^{(j)}\right\}R(t-mT_c-\tau_j)-\frac{1}{2}n_Q'(t), \tag{36}$$

with

$$R(t)=h(t)*h(-t)=\int_{-\infty}^{\infty}|H(f)|^2\cos(2\pi ft)\,df. \tag{37}$$

In the equation above, '*' denotes the convolutional processing and $H(f)$ is the Fourier transform of $h(t)$. The noise components, $n_I'(t)$ and $n_Q'(t)$, represent the lowpass-filtered Gaussian noise processes, which are expressed as

$$n'_I(t) = n_I(t) * h(-t)$$
$$n'_Q(t) = n_Q(t) * h(-t). \tag{38}$$

Sampling the outputs and then multiplying the *i-th* user's I/Q PN sequences, we obtain

$$y_{I,n}=u_I(nT_c)a_{I,n}^{(i)}+u_Q(nT_c)a_{Q,n}^{(i)}$$
$$y_{Q,n}=u_I(nT_c)a_{Q,n}^{(i)}-u_Q(nT_c)a_{I,n}^{(i)}. \tag{39}$$

Given $x_n^{(i)}$ and φ_i, the means and variances of the I/Q channel outputs are given as follows,

$$E\left[y_{I,n}\middle|x_n^{(i)},\varphi_i\right]=\sqrt{E_c^{(i)}}x_n^{(i)}R(\tau_{e,i})\cos\varphi_i$$
$$E\left[y_{I,n}\middle|x_n^{(i)},\varphi_i\right]=\sqrt{E_c^{(i)}}x_n^{(i)}R(\tau_{e,i})\sin\varphi_i$$
$$\mathrm{var}\left[y_{I,n}\middle|x_n^{(i)},\varphi_i\right]=\sigma_{I,I}^2+\sigma_{MA,I}^2+\sigma_{N,I}^2=I_o/2$$
$$\mathrm{var}\left[y_{Q,n}\middle|x_n^{(i)},\varphi_i\right]=\sigma_{Q,Q}^2+\sigma_{MA,Q}^2+\sigma_{N,Q}^2=I_o/2, \tag{40}$$

where $\tau_{e,i}$ is the timing error. $\sigma^2_{I,I}$, $\sigma^2_{MA,I}$, and $\sigma^2_{N,I}$ represent the power spectral density of I-channel due to the inter-chip interference, other-user interference, and background noise, which are given by

$$\sigma_{I,I}^2=\frac{1}{4}E_c^{(i)}E\left[\left\{\sum_{m\neq n}x_m^{(i)}\left\{\left(\cos\varphi_i a_{I,m}^{(i)}+\sin\varphi_i a_{Q,m}^{(i)}\right)a_{I,n}^{(i)}\right.\right.\right.$$

$$+\left(-\sin\varphi_i a_{I,m}^{(i)}+\cos\varphi_i a_{Q,m}^{(i)}+\right)a_{Q,n}^{(i)}\Big\}R(nT_c-mT_c-\tau_{e,i})\Big\}^2$$

$$\left|x_n^{(i)},\varphi_i\right]=\frac{1}{2}E_c^{(i)}\sum_{\substack{m=-\infty\\ m\neq 0}}^{\infty}\left[R(mT_c-\tau_{e,i})\right]^2,$$

$$\sigma_{MA,I}^2=\frac{1}{4}E\Bigg[\Bigg\{\sum_{j\neq i}^{N_u}\sqrt{E_c^{(j)}}\sum_m x_m^{(j)}\Big\{\left(\cos\varphi_j a_{I,m}^{(j)}+\sin\varphi_j a_{Q,m}^{(j)}\right)a_{I,n}^{(i)}$$

$$+\left(\cos\varphi_j a_{Q,m}^{(j)}-\sin\varphi_j a_{I,m}^{(j)}\right)a_{Q,n}^{(i)}\Big\}R(nT_c-mT_c-\tau_{e,j})\Bigg\}^2$$

$$\left|x_n^{(i)},\varphi_i\right]=\frac{1}{2}\sum_{j\neq i}^{N_u}E_c^{(j)}\sum_{m=-\infty}^{\infty}\left[R(mT_c-\tau_{e,j})\right]^2=\frac{1}{2}\sum_{j\neq i}^{N_u}E_c^{(j)},$$

$$\sigma_{N,I}^2=\frac{1}{2}E\left[\left\{n_I'(nT_c)a_{I,n}^{(i)}+n_Q'(nT_c)a_{Q,n}^{(i)}\right\}^2\left|x_n^{(i)},\varphi_i\right.\right]$$

$$=\frac{1}{2}N_o, \tag{41}$$

with the pulse shaping filter normalized, that is,

$$R(0)=\int_{-\infty}^{\infty}|H(f)|^2df=1. \tag{42}$$

Similarly, we can obtain the inter-chip interference, other-user interference, and background noise of Q-channel, which are given by

$$\sigma_{I,Q}^2=\frac{1}{2}E_c^{(i)}\sum_{\substack{m=-\infty\\ m\neq 0}}^{\infty}\left[R(mT_c-\tau_{e,i})\right]^2,$$

$$\sigma_{MA,Q}^2=\frac{1}{2}\sum_{j\neq i}^{N_u}E_c^{(j)},$$

$$\sigma_{N,Q}^2=\frac{1}{2}N_o. \tag{43}$$

Therefore, ignoring the polarity of the information bit for the case of code acquisition, $y_{I,n}$ and $y_{Q,n}$ can be modeled as [11]

$$y_{I,n}=\sqrt{E_c^{(i)}}R(\tau_{e,i})\cos\varphi_i+n_{I,n},$$
$$y_{Q,n}=\sqrt{E_c^{(i)}}R(\tau_{e,i})\sin\varphi_i+n_{Q,n}, \tag{44}$$

where $n_{I,n}$ and $n_{Q,n}$ are the samples of low-pass-filtered Gaussian noise processes each having a variance of $I_o/2$. Since the inter-chip interference is quite small compared to other-user interference and thermal noise, it follows that [11]

$$I_o\approx\sum_{j\neq i}^{N_u}E_c^{(j)}+N_o. \tag{45}$$

After coherent accumulation over N PN chips, Y_I and Y_Q have means and variances

$$E[Y_I|\varphi_i]=N\sqrt{E_c^{(i)}}R(\tau_{e,i})\cos\varphi_i,$$
$$E[Y_Q|\varphi_i]=N\sqrt{E_c^{(i)}}R(\tau_{e,i})\sin\varphi_i,$$
$$\mathrm{var}(Y_I)=\mathrm{var}(Y_Q)=NI_o/2. \tag{46}$$

Therefore, the mean of Z is given by

$$E[Z]=E\left[Y_I^2+Y_Q^2\right]$$
$$=N^2E_c^{(i)}R^2(\tau_{e,i})+NI_o. \tag{47}$$

References

1. W. C. Y. Lee, "Overview of cellular CDMA," *IEEE Trans. on Vehicular Technology*, vol. 40, No. 2, pp.291~302, May 1991.
2. R. L. Pickholtz, L. B. Milstein, and D. L. Schilling, "Spread spectrum for mobile communications," *IEEE Trans. on Vehicular Technology*, vol. 40, No. 2, pp.313~322, May 1991.
3. K. S. Gilhousen, I. M. Jacobs, R. Padovani, A. J. Viterbi, L. A. Weaver, and C. E. Wheatly, "On the capacity of a cellular CDMA system," *IEEE Trans. on Vehicular Technology*, vol. 40, No. 2, pp.303~312, May 1991.
4. E. Sourour and S. C. Gupta, "Direct-sequence spread-sprectrum parallel acquisition in nonselective and frequency-selective Rician fading channels," *IEEE Journal on Selected Areas in Communications*, vol. 10, No. 3, pp.535~544, April 1992.
5. E. Sourour and S. C. Gupta, "Direct-sequence spread-sprectrum parallel acquisition in a fad-

ing mobile channel," *IEEE Trans. on Commun.*, vol. COM-38, No. 7, pp.992~998, July 1990.

6. A. Polydoros and C. L. Weber, "A unified approach to serial search spread-spectrum code acquisition - part Ⅰ and Ⅱ," *IEEE Trans. on Commun.*, vol. COM-32, No. 5, pp.265~283, May, 1984.
7. J. K. Holmes and C. C. Chen, "Acquisition time performance of PN spread-spectrum systems," *IEEE Trans. on Commun.*, vol. COM-25, No. 8, pp.778~784, August 1977.
8. D. M. Dicarlo and C. L. Weber, "Statistical performance of single dwell serial synchronization systems," *IEEE Trans. on Commun.*, vol. COM-28, No. 8, pp.1382~1388, August 1980.
9. M. K. Simon, J. K. Omura, R. A. Scholtz, and B. K. Levitt, Spread spectrum communications, vol. Ⅲ, Ch. 1, 1985.
10. *TIA/EIA Interim Standard* (IS-95), Ch. 6, 1993.
11. A. J. Viterbi, CDMA : *Principles of spread spectrum communication*, Ch. 2~4, Addison-Wesley, 1995.
12. J. G. Proakis, *Digital communications*, 2nd Ed., Ch. 7, McGraw-Hill, 1989.
13. D. Parsons, *The mobile radio propagation channel*, Chs. 5 and 6, John Wiley & Sons Inc., 1992.
14. N. L. Johnson and S. Kotz, *Distributions in statistics : continuous univariate distributions*, vol. Ⅰ and Ⅱ., John Wiley & Sons Inc., 1970.
15. R. E. Ziemer and R. L. Peterson, *Digital communications and spread spectrum systems*, Ch. 7, Macmillan, 1985.

朴 亨 來(Hyung-Rae Park) 정회원

1960년 10월 25일생
1982년 2월 : 한국항공대학 전자공학과 졸업(학사)
1985년 8월 : 연세대학교 대학원 전자공학과 졸업(석사)
1993년 : Syracuse Univ. 전자공학과 졸업(박사)
1985년 9월~현재 : 한국전자통신연구소 선임연구원
※주관심 분야 : 레이다신호처리 방향탐지, 디지탈통신, 대역확산통신 등

康 法 周(Bub-Joo Kang) 정회원

1961년 8월 20일생
1983년 2월 : 경희대학교 전자공학과 졸업(공학사)
1985년 8월 : 연세대학교 대학원 전자공학과(공학석사)
1992년 3월~현재 : 연세대학교 대학원 전자공학과 박사과정
1988년 2월~현재 : 한국전자통신연구소 선임연구원